

## Numerical analysis of polarization maintaining holey fibers with Bragg gratings.

M. Antkowiak<sup>ab</sup>, R. Kotynski<sup>a</sup>, T Nasilowski<sup>a</sup>, F. Berghmans<sup>ab</sup> and H. Thienpont<sup>a</sup>

<sup>a</sup> Vrije Universiteit Brussel, Pleinlaan 2, B-1050 Brussels, Belgium

<sup>b</sup> SCK.CEN, Boeretang 200, B-2400 Mol, Belgium

*We analyze spectral characteristics of Bragg gratings written in index-guiding air-silica holey fibers. In particular, we focus on highly birefringent holey fibers with elliptical holes in hexagonal lattice. We apply Coupled Mode Theory combined with fully vectorial mode solver based on the plane-wave method. We observe large differences in interaction with the grating for the two linearly polarized fundamental modes. Our approach provides an efficient tool to predict spectral characteristics of the fiber Bragg grating-based devices, such as fiber Bragg grating sensors.*

### Introduction

In this paper we investigate holey fibers with Bragg gratings [1] - an architecture which combines two interesting ideas. On one hand there is Bragg grating [2,3], a tool which has been thoroughly studied and successfully applied for the last decade, on the other – holey fiber with its many, not yet precisely known, possibilities. One of the advantages of holey fibers is the relatively large number of design parameters, which can be used to tailor the behaviour of the guided light. In particular, key characteristics of the modes, such as field distribution and effective refractive index, can be adjusted to a specific application.

As it was shown [4], the level of the dopant in the core has a strong impact on the shape of the modes and, consequently, may weaken the properties which are unique to holey fibers. Therefore it can be beneficial to keep the difference of the refractive indices low. Nevertheless, in strong contrast with earlier approaches [5], we do not try to avoid a considerable difference in index of refraction as is normally done by co-doping the photosensitive core with index-lowering dopants such as fluorine.

### Coupling coefficients

To find the number of guided modes and their field distributions, we apply our vectorial numerical mode solver based on the plane-wave method [6]. We model the interaction between the propagating modes and the Bragg grating using the coupled-mode theory [2]. First we calculate the transverse coupling coefficients:

$$\kappa_{ij}^t(z) = \frac{\omega}{4} \iint_{\infty} dx dy \Delta \varepsilon(x, y, z) \vec{e}_i^t(x, y) \cdot \vec{e}_j^t(x, y)$$

where  $e_i^t(x, y)$  and  $e_j^t(x, y)$  are normalized modal transverse field distributions,  $\omega$  is the incident wave's frequency and  $\Delta \varepsilon$  is the perturbation of the permittivity. In many cases, for example when the core consists of a uniformly doped circular rod, this overlap integral can be calculated analytically using the Fourier transform of  $\Delta \varepsilon$ . This allows us to use directly the plane-wave representation of the fields, which improves speed and accuracy of the calculations.

Using the synchronous approximation [2,3] we can describe the coupling efficiency by means of the transverse coupling constant where the permittivity perturbation  $\Delta\varepsilon$  is averaged over the grating period:

$$\kappa_{ij}^t = \frac{\omega}{4} \iint_{\infty} dx dy \overline{\Delta\varepsilon(x, y)} \vec{e}_i^t(x, y) \cdot \vec{e}_j^t(x, y)$$

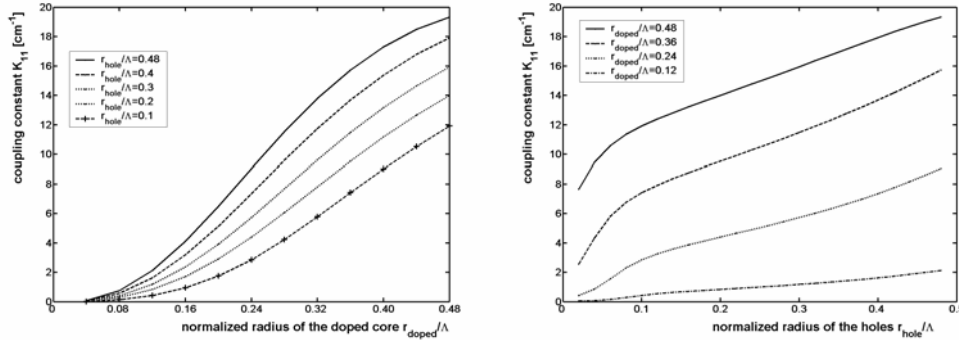


Fig.2 Normalized transverse coupling constant vs. a) hole radius for various radii of the doped-core. b) doped core radius for various radii of the holes. In all structures the hole spacing was  $\Lambda=5\mu\text{m}$ .

Figure 2 shows examples of results for transverse coupling constants between forward- and backward-propagating fundamental modes in a typical holey fiber. For the simulation we used fibers with hole spacing of  $\Lambda=5\mu\text{m}$ , various fill factors and various radii of the doped core. All presented results are obtained for the wavelength of  $\lambda=1.55\mu\text{m}$ . The first graph (Fig.2a) presents the relation between the coupling constant and the radius of the doped core. From this graph it is clear that the efficiency of coupling is increased when the doped region is extended, which is predictable since larger area of the mode interacts with the grating. More interesting results are presented in Fig.2b. It is evident that a targeted coupling efficiency can be achieved not only by extension of the doped area (switching to a higher curve on the graph), but also by increase of the fill factor (moving along one of the curves on the graph). However, it is important to notice that when a single-mode fiber is required, only the configurations with sufficiently small holes can be taken into consideration. In that situation a higher density of the dopant or a larger photosensitive area are good solutions.

## Characteristics of Bragg gratings

Solving the coupled-mode equations we obtain information about the key characteristics of Bragg gratings, such as reflectivity, bandwidth, wavelength corresponding with maximum reflectivity, etc. Characteristic examples calculated for a sinusoidal grating written in two single-mode holey fibers with the same geometry but different radii of the doped core are presented in Figure 3. It is worth noticing that, although the concentration of the dopant is rather low (refractive index of doped silica  $n_{\text{doped}}=1.449$ ) the efficiency of the coupling is strong enough to provide a 100% reflectivity from a few millimeters long grating.

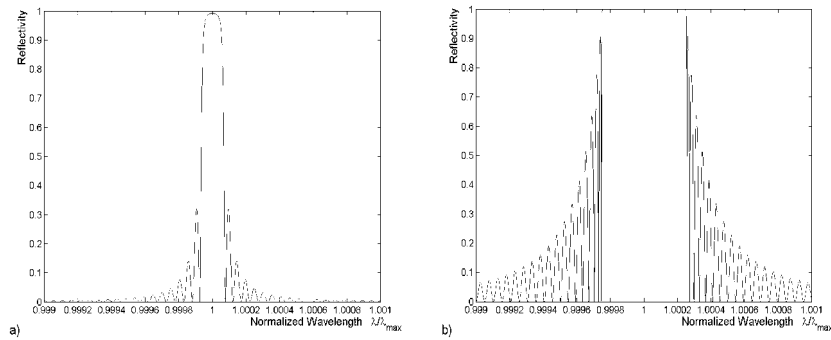


Fig.3 Reflectivity characteristics of a Bragg grating written in a single-mode HF ( $\Lambda=5\mu\text{m}$ ,  $r_{\text{hole}}=0.9\mu\text{m}$ ,  $n_d=1.449$ ) with the radius of the doped core of a)  $r_{\text{doped}}=1.3\mu\text{m}$ . b)  $r_{\text{doped}}=2.1\mu\text{m}$ . Grating was tuned to the wavelength of  $\lambda_{\text{max}}=1.55\mu\text{m}$ .

### Highly Birefringent Hole Fiber with Bragg grating

Having in mind applications in sensing we investigate properties of highly birefringent (polarization maintaining) hole fibers with Bragg gratings. In particular we model index-guiding hole fiber with hexagonal lattice of elliptical holes (Fig 4a). The lattice constant was set to  $\Lambda=0.75\mu\text{m}$ , fill factor  $f=0.21$ , ellipticity  $e=3$ , refractive index of the doped region  $n_{\text{doped}}=1.449$ .

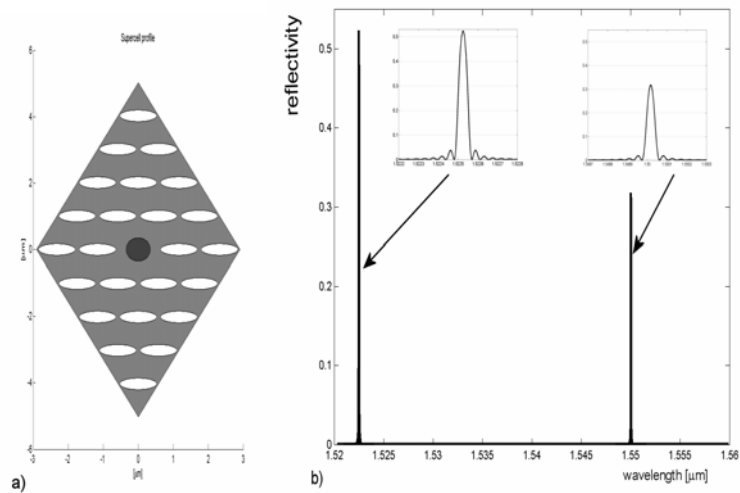


Fig.4 Highly birefringent hole fiber with elliptical holes in hexagonal lattice ( $\Lambda=0.75\mu\text{m}$ , fill factor=0.21, ellipticity=3,  $n_d=1.449$ ). Grating was tuned to the wavelength of  $\lambda_{\text{max}}=1.55\mu\text{m}$ . a) profile of the supercell b) reflectivity from the grating. Two peaks separated by 28 nanometers correspond with two linearly polarized fundamental modes.

A sinusoidal Bragg grating was tuned to the wavelength of  $\lambda_{\text{max}}=1.55\mu\text{m}$ . Since the six-fold symmetry is broken, the degeneracy in propagation constants for two “linearly” polarized fundamental modes is removed. The achieved birefringence of  $B=10^{-2}$  for  $\lambda=1.55\mu\text{m}$ , opens many possibilities for various polarization-based applications. As Figure 4.b shows, the spectral maxima corresponding with two polarizations are well separated by about 28 nanometers. Moreover, the coupling constants are significantly different  $K_{11}/K_{22}=0.69$  which results in the ratio of maximum reflectivities equal to 0.6.

## Conclusions

As we show, the coupling efficiency mainly depends on three factors: the area of the doped core, the concentration of the dopant and the level to which the modes are confined to the core area. The latter can be controlled by choosing the proper geometry of the fiber cross-section, in particular the fill factor. When the size of the holes in the cladding is increased, the energy of the fundamental modes is better concentrated in the doped core, which results in stronger coupling. However, such fibers may be no longer single-mode [7,8]. Hence, an architecture appropriate for a specific application (e.g. fiber sensor) must be a trade-off between the number and the shape of the modes and the efficiency of their coupling with the Bragg grating. Our method provides a tool to find this balance and to predict the spectral characteristics of a device based on the fiber Bragg grating, such as fiber Bragg grating sensors. This approach is complementary with the experimental method of determining the modal properties of a fiber based on the analysis of the inter-mode coupling introduced by a Bragg grating [1,9].

An important observation comes from simulation of highly birefringent holey fiber. The two polarized fundamental modes couple with substantially different efficiencies. Consequently, the reflectivity spectra have different shapes. This fact may be used in many applications, such as sensing. Moreover, this difference should be further increased when the fiber is exposed to external influence (e.g. stress or temperature). We will investigate this phenomenon in the nearest future.

## Acknowledgments

We acknowledge the funding from IAP Photon Network, FWO, GOA, and the OZR of the Vrije Universiteit Brussel.

## References

- [1] B.J. Eggleton, P.S. Westbrook, R.S. Windeler, S.Spälter and T.A. Strasser: Grating resonances in air-silica microstructured optical fibers, *Optics Letters* Vol. 24, pp. 1460-1462, 1999
- [2] T. Erdogan: Fiber grating spectra, *J. Lightwave Technol.*, vol. 15, pp. 1277-1294, 1997
- [3] R. Kyashap: *Fiber Bragg Gratings*, Academic Press, 1999
- [4] T. Nasilowski, R. Kotynski, M. Antkowiak, F. Berghmans and H. Thienpont: Mode analysis of doped-core holey fibers, in *Proc. Of European Symposium on Photonic Crystals*, vol. 1, pp. 133-135, 2002
- [5] J. Riishede, K.G. Hougaard, E.B. Libori, T. Sondergaard, A. Bjarklev: Bragg gratings in Index-guiding photonic crystal fibres, presented at the ECOC 2002, Copenhagen, Denmark, September 8-12, 2002, Paper 3.4.4
- [6] R. Kotynski, T. Nasilowski and H. Thienpont: Vectorial mode characterization of microstructured optical fibers, *Proc. Of the Annual Symposium of the IEEE/LEOS Benelux Chapter*, pp. 187-190, 2002
- [7] N.A. Mortensen: Effective area of photonic crystal fibers, *Optics Express*, vol. 10, pp. 341-348, 2002
- [8] T.A. Birks, J.C. Knight and P.S. Russell: Endlessly single-mode photonic crystal fiber, *Optics Letters* Vol. 22, pp. 961-963, 1997
- [9] C.E. Kerbage, B.J. Eggleton, P.S. Westbrook and R.S. Windeler: Experimental and scalar beam propagation analysis of an air-silica microstructure fiber, *Optics Express*, vol. 7, pp. 113-122, 2000